Supplemental Material can be found at:
http://www.jbc.org/content/suppl/2005/05/05/M500679200.DC1.html

THE JOURNAL OF BIOLOGICAL CHEMISTRY
Vol. 280, No. 26, Issue of July 1, pp. 24553–24561, 2005
© 2005 by The American Society for Biochemistry and Molecular Biology, Inc.
Printed in U.S.A.

Molecular Mapping of Functionalities in the Solution Structure of Reduced Grx4, a Monothiol Glutaredoxin from *Escherichia coli**

Received for publication, January 19, 2005, and in revised form, April 4, 2005
Published, JBC Papers in Press, April 18, 2005, DOI 10.1074/jbc.M500679200

Malin Fladvad‡, Massimo Bellanda§, Aristi Potamitou Fernandes‡, Stefano Mammi§, Alexios Vlamis-Gardikas‡, Arne Holmgren‡, and Maria Sunnerhagen‡¶‖

From the ‡Department of Medical Biochemistry and Biophysics, Karolinska Institutet, S-171 77 Stockholm, Sweden, the §Department of Chemical Sciences, University of Padova, 35131 Padova, Italy, and the ¶Division of Molecular Biotechnology, IFM, Campus Valla, Linköping University, S-581 83 Linköping, Sweden

The ubiquitous glutaredoxin protein family is present in both prokaryotes and eukaryotes, and is closely related to the thioredoxins, which reduce their substrates using a dithiol mechanism as part of the cellular defense against oxidative stress. Recently identified monothiol glutaredoxins, which must use a different functional mechanism, appear to be essential in both *Escherichia coli* and yeast and are well conserved in higher order genomes. We have employed high resolution NMR to determine the three-dimensional solution structure of a monothiol glutaredoxin, the reduced *E. coli* Grx4. The Grx4 structure comprises a glutaredoxin-like α-β fold, founded on a limited set of strictly conserved and structurally critical residues. A tight hydrophobic core, together with a stringent set of secondary structure elements, is thus likely to be present in all monothiol glutaredoxins. A set of exposed and conserved residues form a surface region, implied in glutathione binding from a known structure of *E. coli* Grx3. The absence of glutaredoxin activity in *E. coli* Grx4 can be understood based on small but significant differences in the glutathione binding region, and through the lack of a conserved second GSH binding site. MALDI experiments suggest that disulfide formation on glutathionylation is accompanied by significant structural changes, in contrast with dithiol thioredoxins and glutaredoxins, where differences between oxidized and reduced forms are subtle and local. Structural and functional implications are discussed with particular emphasis on identifying common monothiol glutaredoxin properties in substrate specificity and ligand binding events, linking the thioredoxin and glutaredoxin systems.

Glutaredoxins are ubiquitous proteins found in most living organisms, from prokaryotes to humans. They employ glutathione (GSH)[1] to catalyze redox-dependent cellular functions, such as transcription and biosynthesis regulation, signal transduction, cell cycle control, and protection against oxidative stress (reviewed in Ref. 1). The glutaredoxin family of proteins is closely related to the thioredoxins, which reduce their substrates using a dithiol mechanism in a coupled system with NADPH and thioredoxin reductase (TrxR) (2). The well conserved thioredoxin fold consists of a five-stranded β-sheet flanked by four α-helices (3), where a hydrophobic surface close to the active site (CGPC) mediates substrate binding. A localized conformational change accompanies oxidation of the dithiol form to the disulfide form (4).

The glutaredoxins can be divided into two subfamilies according to their active sites: the classic dithiols, with CP*X*C as the active site and the more recently identified monothiol glutaredoxins, having C*X*F*X* as their suggested active site (1, 5, 6). Careful characterization of dithiol glutaredoxins shows that their main function is the reduction of functionally important protein disulfides, leading to activation and/or inactivation of biological activity. Glutaredoxin targets include the active site of ribonucleotide reductase (reviewed in Refs. 1 and 7), which is essential for DNA synthesis, a disulfide in 3′-phosphoadenylyl sulfate reductase (8), the key enzyme in the reduction of sulfate to sulfite (sulfur assimilation), and the mixed disulfide between arsenate reductase and glutathione forming upon reduction of arsenate to arsenite ions (9). Glutaredoxins can also maintain the activity of redox-sensitive proteins by deglutathionylating cysteines that may form mixed disulfides with glutathione upon oxidative conditions resulting in loss of biological activity (10, 11). Several three-dimensional structures of dithiol glutaredoxins have been determined (10, 12–15). All of these glutaredoxins contain a thioredoxin-like α-β fold where the CP*X*C motif extends from the core in a loop-like structure, and the central β-sheet is composed of four strands compared with the five strands in thioredoxins (reviewed in Ref. 1). Glutathione binding sites have been characterized in atomic detail for human Grx1, *Escherichia coli* Grx1, and *E. coli* Grx3, all of which involve covalent linkage of glutathione to the N-terminal cysteine in the active site loop (16–18). Furthermore, dithiol glutaredoxins share the common property of reducing small molecular weight disulfides with GSH, as shown in the HED assay (17, 18).

Recent studies indicate that, despite significant sequence

* This investigation was supported by grants from the Carl Trygger foundation, the Greek Ministry of Science and Technology (programme Enter), Karolinska Institute, Knut and Alice Wallenberg Foundation, Linköping University, the University of Padova, the Swedish Research Council, the Swedish Cancer Society, the Swedish Child Cancer Society, and the Swedish Society for Medical Research. The costs of publication of this article were defrayed in part by the payment of page charges. This article must therefore be hereby marked "*advertisement*" in accordance with 18 U.S.C. Section 1734 solely to indicate this fact.

[S] The on-line version of this article (available at http://www.jbc.org) contains supplemental Fig. A.

The atomic coordinates and structure factors (code 1YKA) have been deposited in the Protein Data Bank, Research Collaboratory for Structural Bioinformatics, Rutgers University, New Brunswick, NJ (http://www.rcsb.org/).

‖ To whom correspondence should be addressed: Tel.: 46-13-286-682; Fax: 46-13-122-587; E-mail: marsu@ifm.liu.se.

[1] The abbreviations used are: GSH, reduced glutathione; Grx, glutaredoxin; HED, β-hydroxyethyl disulfide; MALDI, matrix-assisted laser desorption/ionization mass spectrometry; Trx, thioredoxin; TrxR, thioredoxin reductase; NOE, nuclear Overhauser effect; HSQC, heteronuclear single quantum coherence; NOESY, nuclear Overhauser effect spectroscopy; TOCSY, total correlation spectroscopy; r.m.s.d., root mean square deviation; GST, glutathione *S*-transferase.

Downloaded from www.jbc.org at Bibl Biologico-Medica, on April 2, 2012

similarities, monothiol glutaredoxin functionality is clearly distinct from that of dithiol glutaredoxins. The monothiol glutaredoxin motif occurs in multidomain arrangements in multicellular eukaryotic species, whereas in lower organisms, only single domain monothiol glutaredoxins have been conserved (19, 20). The monothiol Grx5 from yeast is localized in the mitochondria and performs thioloxidoreductase activity through deglutathionylation of carbonic anhydrase III (21–23). Yeast Grx5 is also required for the activity of Fe-S cluster enzymes (21), which suggests a role in protecting the cell against oxidative stress by regulating the activity of Fe-S cluster proteins. A *Plasmodium falciparum* multidomain protein with a monothiol glutaredoxin domain reduces insulin dimers (22). Neither of these monothiol glutaredoxins reduce small molecular weight disulfides with GSH, and thus appear to lack the classic glutaredoxin activity (22, 23). Furthermore, no substrate has been found for any of these proteins. Among eukaryotic proteins, the human PICOT protein, which is important in oxidative stress response (20, 24), contains two monothiol glutaredoxin domains, but their specific functions are still unknown.

The only monothiol glutaredoxin in *E. coli*, glutaredoxin 4 (Grx4), was recently classified as being essential in a gene footprinting study (25). In agreement with this, several attempts to produce a knock-out of the gene have failed, which indicates that cells lacking Grx4 are not viable (5). Recombinantly expressed Grx4 (115 amino acids) is well folded and thermally stable, with similar biophysical properties as Grx1 (5). Grx4 lacks classic glutaredoxin activity toward small disulfides, and other known substrates for glutaredoxins or thioredoxins such as HED, insulin, and 3′-phosphoadenylyl sulfate reductase are not targets for this essential glutaredoxin (5). Grx4 also differs from the classic glutaredoxins by being a substrate for thioredoxin reductase and not for glutathione (5). However, Grx4 can be glutathionylated and is deglutathionylated with high selectivity by Grx1 (5). Thus, Grx4 is redox-active, but with high substrate specificity. This may explain both why normal dithiol glutaredoxins cannot compensate for the activity of the Grx4 monothiol species in *E. coli*, as was observed for Grx5 in yeast (6), and why the *E. coli* Grx4 monothiol is essential for cell growth and viability.

Despite the close sequence homology between the monothiol and dithiol glutaredoxins, the functionality of the monothiol glutaredoxins remains elusive. In particular, the essentiality of the monothiol glutaredoxins, despite their lack of observable activity in the standard glutaredoxin assays (5), is intriguing. The distinct functionalities displayed by the monothiol glutaredoxins suggests that structural modeling of monothiol glutaredoxins using a dithiol template (19) will not adequately predict functionalities of this novel motif. To further characterize the properties of essential monothiol glutaredoxins, we have employed high resolution NMR to determine the three-dimensional structure of a monothiol glutaredoxin, the reduced *E. coli* Grx4, which is described in this work. Structural and functional implications of the monothiol fold are discussed and analyzed with particular emphasis on substrate specificity and binding events.

MATERIALS AND METHODS

Protein Expression and Sample Preparation—Unlabeled Grx4 was overexpressed in *E. coli* strain BL21(DE3)*grxA*$^-$*grxB*$^-$*grxC*$^-$ using the T7 polymerase/promoter system (pET-15b), as described previously (5). Isotopically labeled Grx4 was produced in rich growth OD2 media from Silantes, containing primary amino acids, some low molecular weight oligopeptides, and almost no carbohydrates. Cells from an overnight culture of unlabeled Silantes OD2 media were spun down, and the pellet was resuspended in ^{15}N- or ^{13}C/^{15}N-labeled Silantes OD2 media containing 100 μg/ml ampicillin. Both unlabeled and labeled protein samples were purified as described earlier (5) and concentrated to 0.75 mM in 125 mM KCl and 5 mM PO_4, pH 6.5.

NMR Measurements and Spectral Evaluation—NMR experiments were performed at 28 °C, using Bruker DMX 600 and Varian Unity INOVA 800 NMR spectrometers. Unlabeled, ^{15}N-labeled, and ^{13}C/^{15}N-labeled proteins were employed. The requirement for KCl in the purification of Grx4 was significant for obtaining spectra with narrow linewidths at near-millimolar protein concentrations. Sequence-specific resonance assignment was obtained from analysis of spin systems and sequential patterns in ^{15}N-^{13}C-HNCA, ^{15}N-HSQC-NOESY, and ^{15}N-HSQC-TOCSY spectra in H_2O, together with analysis of homonuclear NOESY (mix 40 ms, 120 ms), TOCSY (mix 100 ms), and COSY spectra in H_2O, and of double-quantum filtered COSY, TOCSY (mix 40 ms) and NOESY spectra in D_2O. NOEs were obtained from NOESY spectra in H_2O and D_2O recorded with 40-ms mixing time at 800 MHz. Coupling constants were derived from HSQC and NOESY cross-peak line-fitting (26) and from the comparison of signal intensities in a pair of constant-time ^{15}N,^{1}H-HMQC spectra recorded with and without decoupling of the J_{HNH_α} coupling (27). NMR data were processed with the program PROSA (28). All spectra were analyzed, and peaks were integrated with the program XEASY (29).

Structure Calculation—The program ARIA1.2 (Ambiguous Restraints for Interactive Assignment) (30), as an extension of CNS1.1, was used to compute the solution structure of Grx4. NOE cross-peaks from the two-dimensional NOESY and three-dimensional NOESY spectra and chemical shift assignments were used as input to ARIA together with 77 backbone ϕ angles, which were constrained to $-60° \pm 20°$, $-120° \pm 40°$, and $-120° \pm 20°$ for small (<5.5 Hz), large (8 ± 1 Hz), and very large (>9 Hz) $^3J_{HNH_\alpha}$ couplings, respectively. Floating chirality assignment was used for all methylene and isopropyl groups with separate chemical shifts. The experimentally determined distance and dihedral-angle restraints were applied in a simulated annealing protocol using the program CNS, where the starting structure consisted of an extended structure with random side-chain conformations. Optimization of the structure calculation protocol for ambiguous distance restraints and violation analysis was performed as previously described (31). The NOEs were calibrated and largely automatically assigned during the structure calculation by ARIA. The NOEs assigned after eight cycles of structure calculation were subjected to a process of manual editing by a careful re-examination of the spectra to improve the quality of the data set used for structure calculations. The new list of 2703 edited NOEs was used as input for a new set of calculations. Finally, backbone torsion angle restraints derived from chemical shifts using TALOS (32) were added to further improve the already converged unique structure. The dihedral angle restraints were taken to be ±2 S.D. values or at least ± 20° from the average values predicted by TALOS. A short molecular dynamics simulation in a thin layer of explicit water was used to refine the final structure ensemble (33). The resulting 20 energy-minimized conformations were selected to represent the NMR structure of Grx4.

Structure Evaluation—The quality of the structures were evaluated using the PROCHECK (34) and WHATCHECK (35) softwares. The structures were displayed and analyzed using the MOLMOL (36) program, which was also, together with PROCHECK, used to calculate root mean square deviation (r.m.s.d.). WHATIF was used to identify hydrogen bonds from structural criteria as well as tentative hydrogen bonds made possible with minor side-chain adjustments (Optimal Hydrogen Bonding Network (35)). The three-dimensional structural similarity was assessed using the programs DALI (37) and VAST (38, 39), and the hits were evaluated using r.m.s.d. divided by the number of aligned residues (r.m.s.d./N_{align}) as described elsewhere (40). The program Consurf (41) was employed to identify functionally important regions on the surface of the protein, based on the phylogenetic relations between close sequence homologues to Grx4.

Protein Data Bank Accession Number—The coordinates of the 20 energy minimized conformers of Grx4 were deposited in the RCSB Protein Data Bank, with the accession number 1YKA.

RESULTS

The Solution Structure of Grx4—The high resolution structure of Grx4 was calculated from experimental constraints (Table I) by the structure calculation program ARIA (30). Grx4 was completely assigned except for the 4 N-terminal residues, for which no amide proton resonance was observed, and Pro^{25}, where no resonances were observed, most likely due to broadening by exchange in *cis-trans* isomerization. The 10 lowest

Downloaded from www.jbc.org at Bibl Biologico-Medica, on April 2, 2012

TABLE I
Structural statistics of Grx4

Structural characteristics for the 10 lowest energy structures of Grx4	
Distance restraints	
Intraresidue	1034
Sequential	607
Medium range, $i-j \leq 5$	374
Long range, $i-j > 5$	688
All unambiguous	2491
All ambiguous	212
Dihedral angles restraints	
$^3J_{HNHa}$-derived ϕ	77
TALOS-derived ϕ,φ	82, 82
r.m.s.d. from ideality[a]	
Bonds (Å)	0.0052 ± 0.0001
Angles (°)	0.75 ± 0.02
Improper ones (°)	1.80 ± 0.11
r.m.s.d. from experimental data[a]	
Unambiguous NOEs (Å)	0.048 ± 0.015
Ambiguous NOEs (Å)	0.056 ± 0.004
All NOEs (Å)	0.049 ± 0.014
Torsion angles constraints (°)	2.08 ± 0.22
Ensemble r.m.s.d. (Å)	
Secondary structure (backbone)[b]	0.56 ± 0.11
Secondary structure (heavy)[b]	1.10 ± 0.10
Backbone (residues 5–115)[b]	0.69 ± 0.09
Heavy atoms (residues 5–115)[b]	1.24 ± 0.08
Ramachandran plot appearance (residue 5–115)[c]	
Most favored regions (%)	83.9
Additionally allowed regions (%)	12.7
Generously allowed regions (%)	3.4
Disallowed regions (%)	0.0

[a] Average values.
[b] Average r.m.s.d. with respect to the mean calculated with MOLMOL (36).
[c] Calculated with PROCHECK-NMR (34).

energy structures were chosen to represent the NMR structure of Grx4 (Fig. 1*A*). An evaluation of the structure statistics of the ensemble (Table I) shows a well defined core domain, where the r.m.s.d. values for the regular secondary structure and the backbone heavy atoms of the ensemble were 0.49 and 0.58 Å, respectively. Within this core domain, which comprises residues 5–115, 84% of the residues are well distributed in the most favored region in the Ramachandran plot. The N-terminal 4 residues were unassigned due to rapid amide exchange and are therefore not included in the structure statistics. Long and medium range NOEs are well distributed over the entire protein (see Supplemental Material).

Grx4 has a glutaredoxin/thioredoxin-like fold, which consists of a four-stranded β-sheet, flanked by five α-helices (Fig. 1*A*). Regular secondary structure elements were identified for residue 5–14 (α_1), 17–21 (β_1), 33–43 (α_2), 48–51 (β_2), 56–66 (α_3), 73–76 (β_3), 79–80 (β_4), 84–93 (α_4), and 95–107 (α_5) in the majority of the NMR conformers. Residues 81–82, together with residue 74, form a structure almost definable as a classic β-bulge, a conserved feature in the corresponding position of the thioredoxin fold, but distances between 74O and 82NH are slightly above the threshold formally required for the formation of a hydrogen bond. Helices α_1 and α_3 are located on the same side of the β-sheet and are oriented orthogonally to each other. Helices α_2, α_4, and α_5 are located on the opposite side of the β-sheet, where α_2 and α_4 are essentially parallel. Helices α_4 and α_5 are almost continuous in sequence but are structurally tilted by 90°, most likely facilitated by the conserved Gly^{94} interspaced between the helices. The C terminus of α_5 is connected to the short loop between β_3 and β_4 through a hydrogen bond involving Tyr^{107} Oη and Asp^{77} O$^{\delta1}$, which may be important in defining the orientation of α_5.

Well ordered side chains (r.m.s.d. < 1) are predominantly found in the core, or are partly buried (Fig. 1*B*). Seven well ordered side chains are exposed (>30%), including Gln^{54} and Pro^{56}, in an exposed loop preceding α_3, Pro^{69}, which is strictly conserved within the monothiol family, and residues 38, 42, 89, and 92, in the exposed C-terminal parts of α_2 and α_4 (Fig. 1*B*). A set of 26 residues with side-chain solvent exposures of <10% defines the core of Grx4 (Fig. 2*A*). This core includes all of β_1, one face of α_2, β_3 and the preceding loop, and the conserved GG glutaredoxin signature sequence (17) (residues 82–83). Residues Ile^8, Ile^{12}, Leu^{62}, Pro^{63}, Val^{87}, Leu^{96}, Ile^{100}, Thr^{103}, and Thr^{104} connect α_1, α_3, α_4, and α_5 to the solvent-excluded core. Residues Leu^{44}, Ile^{52}, and Asp^{113} are buried but do not form part of any secondary structure element.

The suggested active site of Grx4 (Cys^{30}–Ser^{33}) is located on the molecular surface, N-terminal to α_2, and appears partially disordered in the structure ensemble. Indeed, NOEs are scarce for both the active site and several preceding residues, which may be due to conformational exchange and/or to the exposed nature of the loop. However, parts of the active site region are rigid, as suggested by the *cis*-conformation adopted by Pro^{72}, which is in close spatial proximity. The *cis*-peptide conformation was deduced from the presence of sequential $d_{\alpha\alpha}$ and the absence of sequential $d_{\alpha\beta}$ NOE between residues 71 and 72. A corresponding *cis*-Pro close to the active site is found in most glutaredoxins/thioredoxins and is thought to play a role in folding and redox dynamics (15). Furthermore, a distinct hydrogen bond between Cys^{30}NH and Lys^{22}O′, and a reciprocal tentative hydrogen bond linking the side-chain amide of Lys^{22} with Cys^{30}O′, could be important in determining the geometry of the C*X*F*X* tetrad and/or of the preceding loop. Indeed, a lysine at the corresponding position is fully conserved in all monothiol glutaredoxins (Fig. 2*A*).

The surface of Grx4 shows two pronouncedly hydrophobic and elongated patches, positioned where the edges of the β-sheet exit from the protein core, but with a direction that is orthogonal to the sheet itself (Fig. 1*C*). Although surrounded by a fairly even distribution of negative and positive charges, these patches are uncommonly large for a single-domain protein, and may reflect the narrow solution conditions accessible to NMR studies. The directional and elongated shape of these surfaces suggests that they could be of functional significance for protein interactions and/or oligomerization.

Structural Evaluation of Conserved Residues in the Monothiol Family—In addition to the conserved tetrad in the predicted active site loop, which is the key feature of the monothiol glutaredoxin family, a set of buried conserved residues in the protein core suggest a conserved sequence basis for a common structural scaffold (Fig. 2*A*). The β_1-α_2-β_3-GG core described above, as well as the buried Ile^{52}, are well conserved in both the monothiol and dithiol glutaredoxin family. Notably, however, the last residue in β_1, which is close to the active site, is strictly Met in the monothiol glutaredoxins, whereas smaller residues (Thr and Gly) are found in the corresponding dithiol position (Fig. 2*A*). An alternative start codon for the monothiol glutaredoxins at this conserved Met is, however, unlikely, because significant parts of the buried core would then not be included. In agreement with this, Grx4$_{21–115}$ is expressed as inclusion bodies (5). Specific monothiol signature motifs include the anchoring of α_3 to the core through a conserved (L/I)(P/K) residue pair, and of α_1 and α_5, helices that are much shorter or nonexistent in the dithiol glutaredoxins, by conserved Ile, Leu, or Val residues. Because these core residues are distinct from the dithiol family, they may be required for the preservation of a monothiol fold.

In addition to the conserved core, several surface residues are nearly identical in sequence throughout the monothiol glutaredoxin family. A Consurf (41) analysis showed that most of

Downloaded from www.jbc.org at Bibl Biologico-Medica, on April 2, 2012

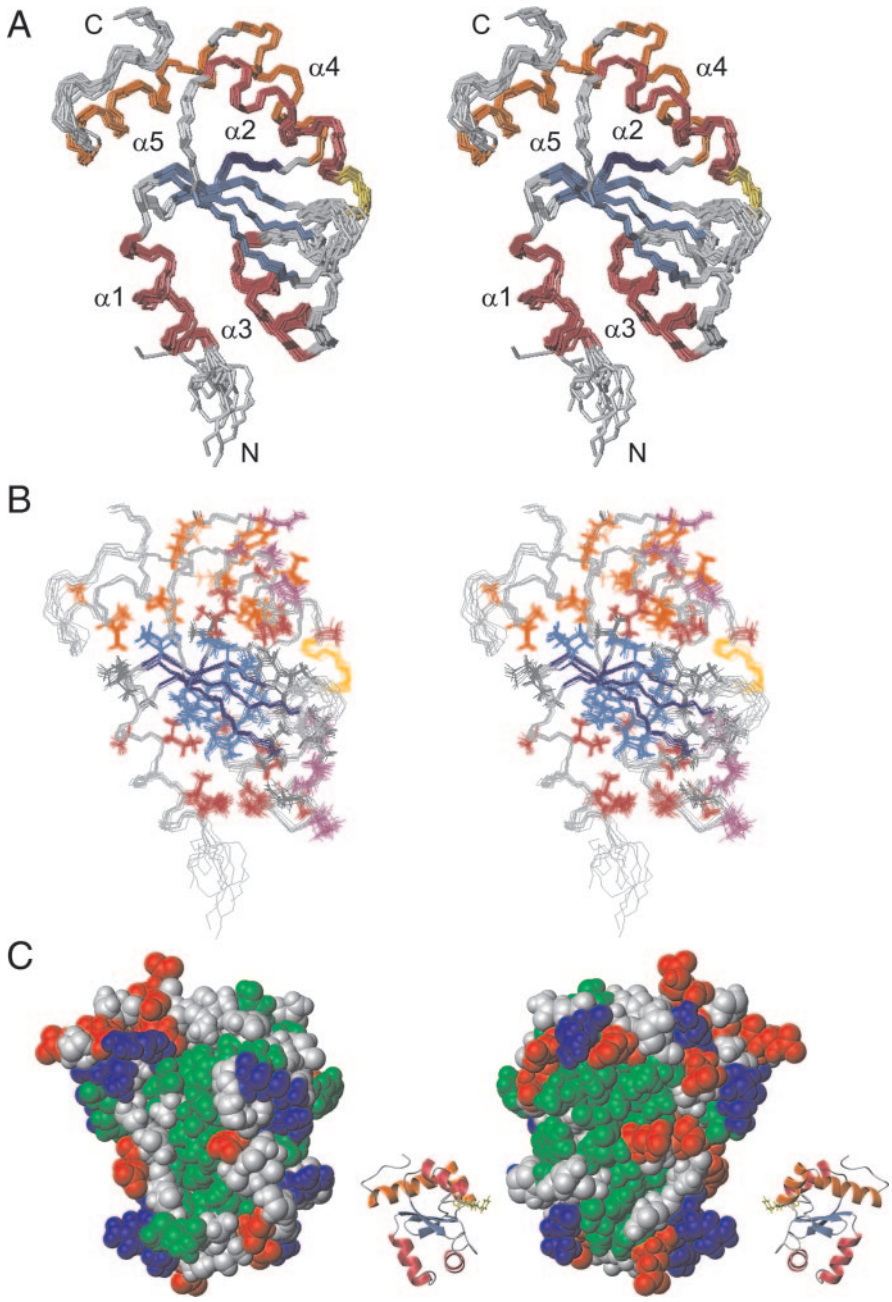

FIG. 1. **Stereoview showing overlay of the ten lowest energy structures of Grx4.** *A*, backbone only. The polypeptide backbone is shown in *gray*, the helices α_1-α_3 in *dark red*, α_4-α_5 in *light red*, and the four strands (ordered β_2, β_1, β_3, and β_4 from the *front of the figure*) in *blue*. The active site is *yellow*, and the residues forming the β-bulge are *navy blue*. *B*, ordered side chains (r.m.s.d. < 1) of residues in Grx4 are displayed as *sticks*. Side chains are colored according to their participation in secondary structure elements as in *A*, except that the seven exposed and ordered side chains are shown in *purple*. The β-sheet backbone is *navy blue*, whereas helices are *gray* to improve the clarity of the figure (*C*). The hydrophobic surface of Grx4 is displayed in *green*, negatively charged residues in *red*, and positively charged ones in *blue*. The orientation of Grx4 in *C* is also displayed as a *schematic*. The graphics were generated using MOLMOL (36).

these exposed residues cluster together on the same face of Grx4 (22, 30–33, 53, 59, 69–71, 85–86, and 89 (Fig. 2*B*)), whereas only very few conserved residues are exposed on the opposite face (Fig. 2*C*). The main cluster of conserved residues is located in direct contact with the suggested active site loop, implying a conserved substrate/ligand binding pocket in the monothiol family (Fig. 2*B*). Conserved surface residues on the opposing Grx4 face (Fig. 2*C*) include residue Ala^{66}, finalizing helix α_3, Glu^{95}, capping helix α_5 and Glu^{79}, critical for forming the short β-sheet β_4, as well as residues 23 and 28, which form part of a surface-exposed loop preceding the active site. Notably, the hydrophobic surface patches of Grx4 are not conserved throughout the monothiol family.

Comparison of Grx4 with Structurally Related Proteins—The structurally closest relatives of the monothiol Grx4 are found among dithiol glutaredoxins and glutathione *S*-transferases (GST) (Fig. 3). Among published structures, the most similar proteins identified by DALI (37) include two dithiol glutaredoxins, glutaredoxin 1 (Grx1) from pig liver (42) (r.m.s.d./N_{align} = 0.029) and glutaredoxin 2 (Grx2) from *E. coli* (r.m.s.d./N_{align} = 0.035) (Fig. 3), as well as several GSTs with structure similar to *E. coli* Grx2. The secondary structure elements and the active sites of Grx4 and Grx1 superimpose well; only the length of the secondary structure elements varies in some parts of the structures. Grx2 from *E. coli* and the GST proteins found in the DALI search have an N-terminal glutaredoxin domain similar to Grx4 as well as an additional C-terminal α-helical domain. The N-terminal glutaredoxin domain of Grx2 aligns well structurally with Grx4, although Grx2 lacks an N-terminal helix found in Grx4, and connects to its C-terminal domain by a loop at the position of α_5 in Grx4. The active site in Grx2 is positioned similarly as the C*X*F*X* monothiol sequence in Grx4, but while the C-terminal domain of Grx2 wraps up close to the side of the glutaredoxin domain, covering the Grx2 active site, the Grx4 monothiol sequence is surface-exposed and partially disordered. A VAST (38, 39) search also ranked Grx1 from pig liver as the structure most similar to Grx4, but also identified Grx3 from *E. coli* (r.m.s.d./N_{align} = 0.031) as a structural ho-

Downloaded from www.jbc.org at Bibl Biologico-Medica, on April 2, 2012

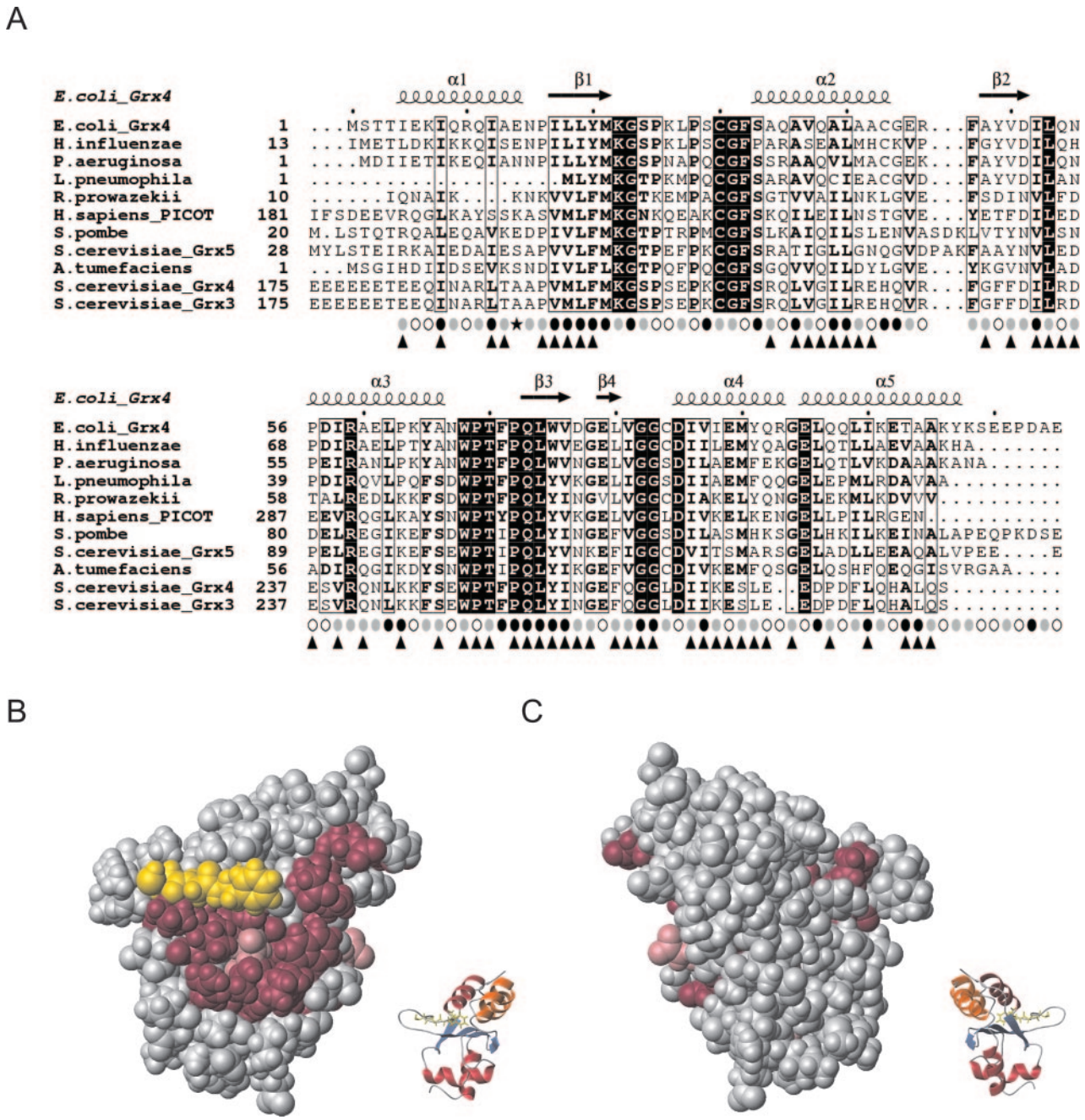

FIG. 2. **Sequence evaluation of proteins containing a monothiol motif.** *A*, Conservation between the sequences is indicated with *black boxes* for strict identity, *bold characters* for similarity within a group of similar amino acids, and *black frames* for similarity across different groups. The sequences were obtained from the Swiss Protein Data base and have the following accession numbers: *E. coli_Grx4* (P37010), *H. influenzae* (P45085), *P. aeruginosa* (Q9HY77), *L. pneumophila* (Q48833), *R. prowazekii* (O05957), *H. sapiens_PICOT* (O76003), *S. pombe* (Q9HDW8), *S. cerevisiae_Grx5* (Q02784), *A. tumefaciens* (Q8UEA6), *S. cerevisiae_Grx4* (P32642), and *S. cerevisiae_Grx3* (Q03835). Below the sequence alignment, side-chain surface exposure as calculated by MOLMOL (*filled circles*: <10%; *gray circles*: 10–30%; *open circle*: >30%), and residues with side-chain r.m.s.d. values <1 (▲) are indicated. Sequences of the multidomain proteins *H. sapiens_PICOT*, *S. cerevisiae_Grx4*, and *S. cerevisiae_Grx3* sequences have been truncated (*). *B* and *C*, the surface amino acid conservation of Grx4 calculated by Consurf, active site in *yellow*, conserved residues in *purple*, conserved substitutions in *pink*, and non-conserved residues in *light gray*. The orientations of Grx4 are indicated by *ribbon representations*, where *B* and *C* are rotated by $z - 180°$ with respect to each other. The alignment was constructed using the programs ClustalW (48) and ESPript (49). The graphics were generated using MOLMOL (36).

mologue. Grx3 from *E. coli* contains all helices but the N-terminal α_1 in Grx4 and instead starts with a β-strand corresponding to β_1 in Grx4. Furthermore, Grx4 is structurally similar to the glutaredoxin domain of peroxiredoxin 5 from *Haemophilus influenza*, two GST proteins, and the human glutaredoxin-like protein SH3BGRL3. The thioredoxin proteins were not identified as closely structurally related to Grx4, most likely because the thioredoxins have an additional N-terminal β-strand not found in Grx4 or other glutaredoxins.

Conserved Surface Features in Grx4 Suggest a Conserved Monothiol Ligand Binding Mode—Although no structure of a glutathionylated monothiol glutaredoxin is yet available, a comparison of the conserved surface features with the glutathione binding pattern of Grx3 (17) and Grx1 (18) suggests that Grx4 adopts a mode of glutathione binding similar that of Grx3. The glutathione binding residues of Grx3 are identical in Grx4 (Fig. 4*A*), despite the relatively low sequence homology of the two proteins (27%). Furthermore, despite the differences in

Downloaded from www.jbc.org at Bibl Biologico-Medica, on April 2, 2012

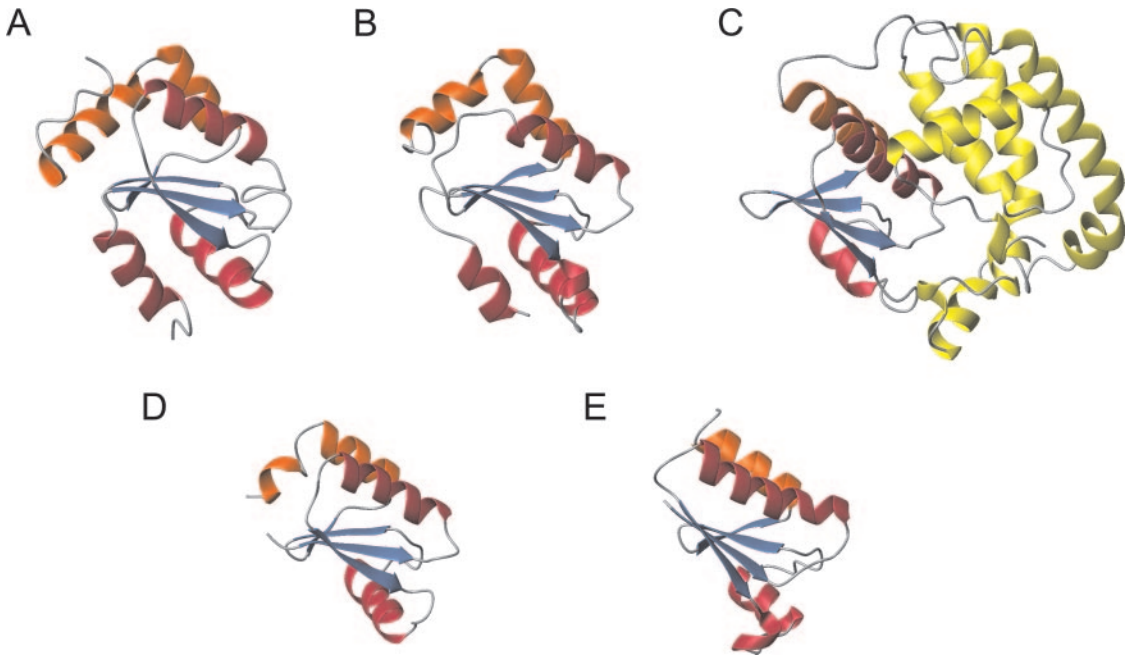

FIG. 3. **Ribbon representation of Grx4 and proteins with high structural similarity.** *A*, Grx4 from *E. coli*; *B*, Grx1 from pig (PDB code 1kte); *C*, Grx2 from *E. coli* (PDB code 1g7o); *D*, Grx3 from *E. coli* (PDB code 3grx); and *E*, Grx1 from *E. coli* (PDB code 1grx). The polypeptide backbone is shown in *gray*, the helices corresponding to α_1-α_3 in Grx4 in *dark red*, α_4-α_5 is *light red*, and the four strands are *blue*. The C-terminal domain of Grx2 is shown in *yellow*. The graphics were generated using MOLMOL (36).

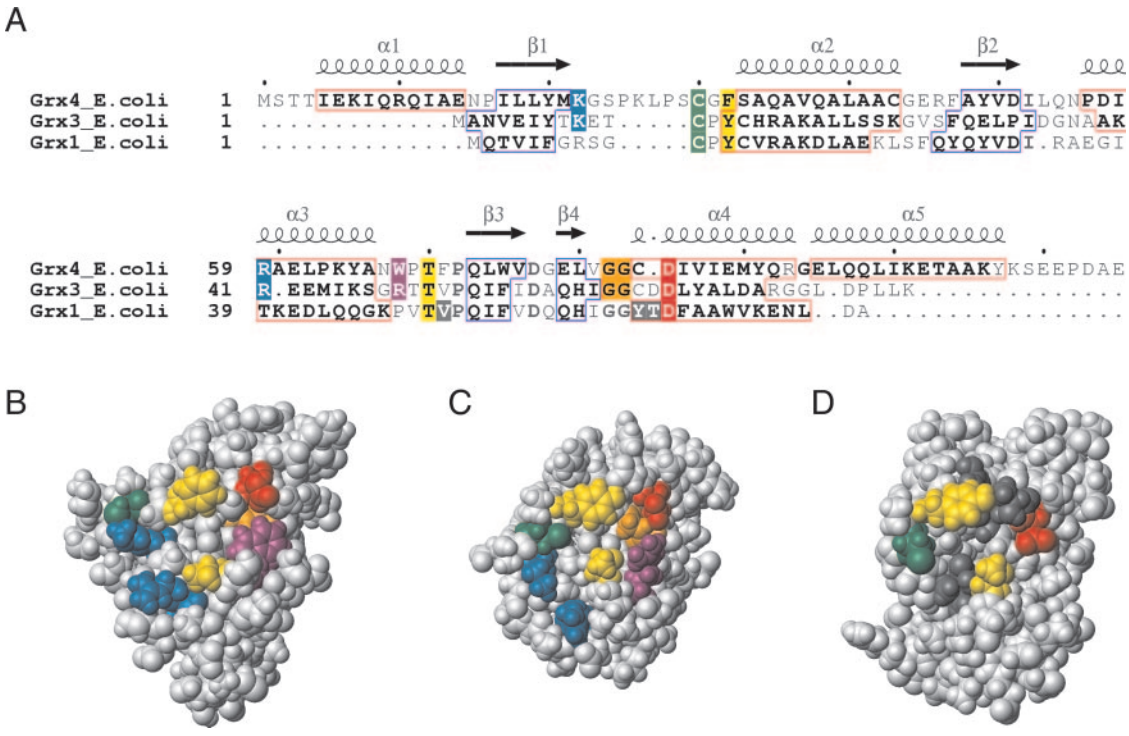

FIG. 4. **Comparison of residues involved in glutathione binding.** *A*, alignment of *E. coli* Grx4, Grx3, and Grx1. Secondary structure in all proteins are displayed on the sequences (α-helices: *red boxes*; β-strands: *blue boxes*), and the labeling of the Grx4 secondary structure elements is at the *top*. Glutathione binding surfaces of Grx4 (suggested) (*B*), *E. coli* Grx3 (17) (*C*), and *E. coli* Grx1 (*D*) (18). Conserved residues are colored according to function: The Cys (*green*) forms a disulfide bond to the glutathione in Grx3 and Grx1, conserved Arg and Lys residues form salt bridges to the C-terminal Gly of glutathione in Grx3 (*blue*) (the corresponding Arg in Grx1 is not involved in ligand binding), a Gly-Gly pair (*orange*), a Thr and a Phe/Tyr (*yellow*) shape the glutathione binding groove on the Grx3 protein surface, and an Asp (*red*) provides complementary charges in Grx3 and Grx1 for γ-Glu_{GS}. Remaining residues involved in glutathione binding in Grx1 are shown in *dark gray*. Grx4 Trp^{68}, which is strictly conserved in monothiol glutaredoxins, and the corresponding residue in Grx3 (Arg^{49}) are displayed in *purple*.

helical extent and relative helix orientations between the two proteins, the relative surface positioning of the conserved glutathione binding residues is remarkably similar and forms a tentative interaction surface of similar size and extent (Fig. 4, *B* and *C*). Only one small difference is notable: whereas in Grx3 the GG motif is exposed and participates in glutathione binding, the same residues in Grx4 are buried and hidden behind the exposed Trp^{68}, which is strictly conserved in monothiol glutaredoxins. In contrast, the glutathione-binding surface of *E. coli* and human Grx1 is significantly more compact and has

Downloaded from www.jbc.org at Bibl Biologico-Medica, on April 2, 2012

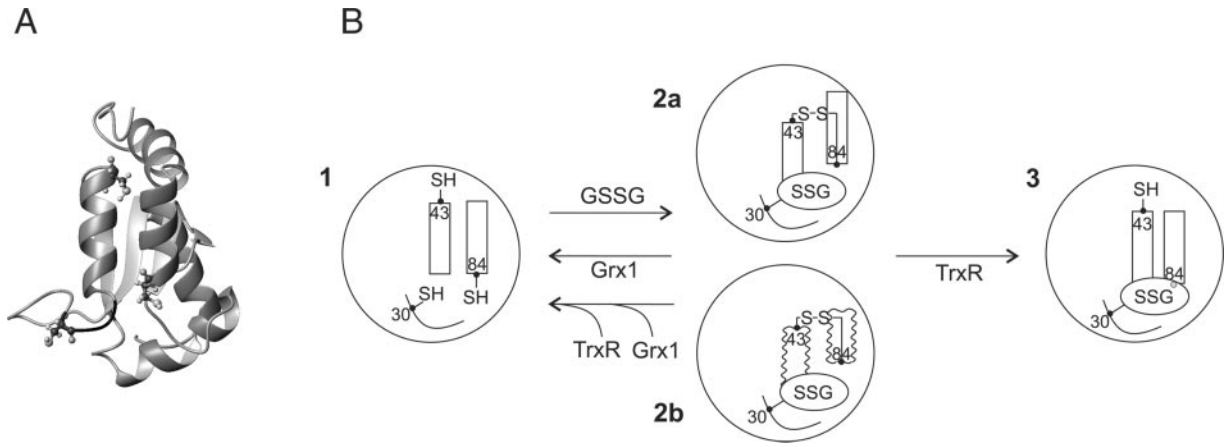

FIG. 5. **Structural interpretation of MALDI results.** *A*, ribbon representation of Grx4 showing the location of the three cysteines (in *ball and stick* representation). *B*, *schematics* showing the oxidation and reduction of Grx4. Reduced Grx4 (*1*) is oxidized by oxidized GSH resulting in formation of one intramolecular disulfide bridge (Cys^{43} and Cys^{84}) and one GS-mixed disulfide on Cys^{30} (*2*). The intramolecular disulfide can be formed either by relative reorientation of α_2 and α_4 (*2a*) or by complete/partial unfolding of α_2 and α_4 (*2b*). Reduction of oxidized Grx4 by TrxR leads to breakage of the intramolecular disulfide (*3*), whereas Grx1 by itself or in combination with TrxR reduces Grx4 completely (*1*).

a more pronounced groove-like appearance (Fig. 4*D*). The strict conservation of the Grx3-like glutathione binding motif (Fig. 2*A*) suggests that monothiol glutaredoxins across a wide range of species bind glutathione similarly, and that Trp^{68} may actively participate in ligand binding.

Structural Evaluation of MALDI Data Describing Changes in Grx4 on Glutathionylation—The careful choice of MALDI experiments, which revealed the activity of thioredoxin reductase on glutathionylated, oxidized Grx4 (5), also reveals important structural features involved in the redox cycle of this protein. Grx4 contains 3 cysteines, one of which is located in the monothiol tetrad (Cys^{30}). Our previous experiments revealed the possibility of disulfide formation on glutathionylation (5). In short, thioredoxin reductase was shown to reduce an internal Grx4 disulfide, but leaving only one cysteine accessible to iodoacetamide (IAM) modification; Grx1 by itself was able to deglutathionylate one Cys in Grx4, leaving one Cys inaccessible; and finally, pre-treating Grx4 with TrxR before adding Grx1 lead to the formation of three free thiols (5).

When interpreted in the context of the present Grx4 structure, the previous MALDI results consistently suggest structural changes on glutathionylation and concomitant disulfide formation (Fig. 5). First, Cys^{30} is assumed to be covalently attached to glutathione, as is highly suggestive based on the conservation of the binding site. The other two cysteines, Cys^{43} and Cys^{84}, must then be disulfide-linked in oxidized Grx4. In the reduced protein, Cys^{43} and Cys^{84} are positioned on the opposite ends of helices 2 and 4, with a distance of 14 Å. The formation of a disulfide on oxidative glutathionylation must therefore be related to a structural change, either by partial unfolding of either or both helices 2 and 4, or by slight relative reorientation of these helices so that the opposing ends come closer to each other (Fig. 5). The reduction by thioredoxin reductase of GS-Grx4 reduces the internal disulfide bond, but cannot remove the glutathione, and allows for IAM modification of only one cysteine (5). In contrast, TrxR treatment of deglutathionylated Grx4 results in IAM modification on all cysteines. In the structure of Grx4, Cys^{84} is close to the suggested glutathione-binding surface, and could well be buried on glutathionylation. Thus, the mono-IAM modification resulting from TrxR treatment of GS-Grx4 is likely due to burial of Cys^{84} on glutathionylation.

DISCUSSION

The quest for the biological function of the monothiol glutaredoxins has been a rational behind the current solution structure determination of Grx4. Accumulating evidence demonstrate that monothiol glutaredoxins are essential in both *E. coli* and yeast (5, 6). Their conserved occurrence in higher order genomes suggests that any common functionality in this subfamily is likely to be of general importance for fundamental biological mechanisms, such as cellular defense against oxidative stress. However, despite several attempts to reveal the functionality of the monothiol glutaredoxins (5, 20, 22–24), their main biochemical activity is still unknown.

The structure of Grx4 allows for a more detailed evaluation of the role of conserved residue patterns in the monothiol family than is possible from sequence alignment alone. First, it is clear that the buried core of Grx4 is nearly identical in all monothiol glutaredoxin sequences identified to date, thus suggesting a closely conserved core-stabilized fold. The structure is closely related to the well known thioredoxin/glutaredoxin fold, including specific local structure patterns such as a conserved β-bulge and a *cis* proline close to the active site. These similarities are also supported by the near-equal thermodynamic properties of Grx4 with the dithiol Grx1 in thermal unfolding experiments (5). Although the extent of secondary structure elements and the number of helices varies considerably within the dithiol thioredoxin/glutaredoxin fold family, all but the monothiol glutaredoxin of *Legionella pneumophila* are predicted to contain helices α1–α5, and the residues in the β-sheet are nearly identical (Fig. 2*A*). Together with the observed high conservation of core residues, where residues from all secondary structure elements participate, the tertiary structure of Grx4 is most likely well conserved within the monothiol glutaredoxin family, perhaps even better conserved than the dithiol glutaredoxin fold.

Surface-conserved residues in the monothiol family form a pronounced surface patch surrounding the C*X*F*X* tetrad. Remarkably, several of these exposed residues are both identical to and have similar structural position as glutathione-interacting residues in the *E. coli* mixed disulfide Grx3-SG, which is formed with the first cysteine in the dithiol CP*X*C active site. Thus, of the 3 cysteines present in Grx4, glutathione should be attached to the cysteine in the C*X*F*X* tetrad. The remarkable surface conservation among monothiols suggests that they are all able to employ the same cysteine to form a mixed disulfide with glutathione. Thus, a common glutathione-interacting mechanism is conservatively built into the monothiol glutaredoxin fold in a wide range of species.

The monothiol glutaredoxins display additionally conserved

Downloaded from www.jbc.org at Bibl Biologico-Medica, on April 2, 2012

residues close to the presumed active site loop, which are likely to contribute to specific monothiol-type glutathione-dependent glutaredoxin activity. These residues include the strictly conserved WP motif, represented in Grx4 by residues Trp^{68} and Pro^{69}, which is absent in Grx3 and indeed in all dithiol glutaredoxins and thioredoxins. On the Grx4 surface, Trp^{68} is located in a similar position as Arg^{49} in Grx3, where the guanidino group provides a complementary charge for the α-carboxylate in γ-Glu_{GS} (17). The side-chain NH of Trp^{68} could fulfill a similar but not identical role in Grx4, most likely resulting in altered glutathione orientation and/or stability. Furthermore, Pro^{69}, its surface neighbor, cannot form hydrogen bonds, in contrast to the corresponding Thr^{50} in Grx3 (17). Thus, although the surface conservation of residues Lys^{22}, Arg^{59}, and Thr^{70} with glutathione-binding residues in Grx3 suggests that the anchoring of the Gly_{GS} is nearly identical in monothiol and dithiol glutaredoxins, the anchoring of the α-carboxylate in γ-Glu_{GS} should be slightly different in monothiol and dithiol glutaredoxins. Furthermore, in the dithiol Grx3, its charged residues Arg^{16} and Asp^{66} as well as Tyr^{13} in the dithiol active site tetrad were suggested to anchor γ-Glu_{GS} upon GSH reduction of Grx-SG in monothiol glutaredoxins, and movement of Tyr^{13}, as observed by the breaking of a hydrogen bond with the phenolic oxygen, was proposed to play an active role in displacing the subsequently formed oxidized GSH from the active site (17). Notably, neither of these residues is conserved in Grx4 (Fig. 4) or in other monothiol glutaredoxins (Fig. 2) suggesting that a second binding site for GSH may be absent. Furthermore, the monothiol C*X*F*X* motif has a Phe in the position corresponding to the suggested active site Tyr in dithiol glutaredoxins, thus precluding the suggested hydrogen-bond switch. Two strictly conserved exposed residues in the monothiol glutaredoxins remain that have no correspondence in Grx3: Ile^{86} and Glu^{89}, which are positioned on the edge of the conserved surface. Possibly, these residues could be involved in specifying novel mechanisms for molecular recognition in the reduction and/or catalytic activity of monothiol glutaredoxin glutathione mixed disulfide complexes, and even be a prerequisite for TrxR reduction.

Although strikingly similar, the small variation in the glutathione-binding surface between monothiol and dithiol glutaredoxins may reflect their difference in functionality. First, Grx4, as well as other monothiol glutaredoxins, does not catalyze the reduction of a GS-β-mercaptoethanol mixed disulfide, as shown by the lack of activity in the HED assay (5, 22, 23). Notably, an engineered monothiol glutaredoxin derived from the dithiol Grx1 (Grx1 C14S) could perform this function (18). Similar results were obtained with the other two glutaredoxins from *E. coli*.[2] This suggests that the reduction of GS-β-mercaptoethanol mixed disulfide requires sequence constraints elsewhere than in the active site tetrad, requirements that may specify the interaction and stability of mixed disulfide transition intermediates. Indeed, the lack of activity of the monothiol yGrx5 in the HED assay has been explained in terms of low reactivity with GSH (23). This is in excellent agreement with the observed lack of surface conservation in the suggested second GSH-binding site, as described above.

The lack of classic glutaredoxin activity in monothiol glutaredoxins could imply that a partner protein would be required for full functionality. This would be in analogy with the GST-like protein *E. coli* Grx2, where the C-terminal helical region has an occluding effect on the active site that is thought to be important for substrate specificity (15). However, surface conservation among monothiol glutaredoxins, which could indicate a binding site for a partner protein, is absent outside the suggested glutathione binding site. This suggests that the monothiol glutaredoxin motif, although part of several multidomain proteins, functions as an individual domain and does not require a conserved partner protein for full function.

Upon glutathionylation of Grx4, an internal disulfide is formed (5). Current MALDI results together with the structure of reduced Grx4 suggest that significant structural changes are involved in oxido-reduction of this monothiol glutaredoxin. Grx4 would require relative repositioning of secondary structure elements and/or partial unfolding, to accommodate the glutathionylation-induced internal disulfide linking between Cys^{43} and Cys^{84}, which are 14 Å apart on opposite ends of α_2 and α_4 in the reduced form. Although a complete structure of the oxidized form of Grx4 is required to understand how this is accomplished, it should be noted that small rotations in the dihedrals of Val^{81} suffice to tilt α_2 and α_4 to allow for disulfide formation between Cys^{43} and Cys^{84}. The movement causes disruption of two hydrogen bonds only, one of which is Tyr^{107}–Asp^{77}. A slight rotation of the Gly^{94} between α_4 and α_5 is sufficient to bring back α_5 to the core. The Val^{81} and Gly^{94} positions are conserved in the genomes of all species with only a single monothiol glutaredoxin motif, whereas in *Saccharomyces cerevisiae*, only Grx5 maintains these conserved positions.

The required magnitude of structural changes on Grx4 oxidation contrasts with previous observations of the human and *E. coli* thioredoxins as well as *E. coli* Grx3, where the changes observed between oxidized and reduced forms are subtle and local (17, 43). Sequence constraints limit Grx4-like disulfide formation on glutathione binding to the *E. coli* and *Haemophilus influenzae* monothiol glutaredoxins (Fig. 2*A*), and the *L. pneumophila* may well form an internal disulfide between residues corresponding to Ala^{39} and Cys^{43} in Grx4 α_2. However, it should be noted that oxidation of 3 cysteines, as in Grx4, is generally a three-step reaction where creation of an intramolecular disulfide via an unstable mixed disulfide intermediate involving two closely situated cysteines is followed by formation of a mixed disulfide on the third cysteine (44). Thus, the structural change on glutathione binding that allows for intradisulfide formation is likely to occur also in other monothiol glutaredoxins. In the several monothiol glutaredoxins with only one or no cysteines outside the CF*X*F tetrad, glutathionylation could still promote further interactions by revealing new interaction patches. Considering that the internal disulfide of *E. coli* Grx4 could be a substrate of TrxR, and, as such, would represent an interface between the thioredoxin and glutaredoxin systems (5), one could even conceive of the region involving these 2 cysteines as an active site region of Grx4. It is therefore interesting that the surface-exposed side chains in the region between the 2 cysteines on the surface of α_2 and α_4 in Grx4 are surprisingly well ordered (Fig. 2*B*). The structure of Grx4 thus suggests that, both from a molecular and biological perspective, the main active region of the monothiol glutaredoxins may be situated elsewhere than in the C*X*F*X* tetrad.

Although the suggested magnitude of structural change in Grx4 on oxidation exceeds that which has previously been observed for dithiol glutaredoxins, recent data have put forward redox mechanisms that involve large changes in quaternary structure. The Zn^{2+}-dependent redox switch domain of the chaperone Hsp33, resembling a nascent thioredoxin-like domain, is proposed to be activated for disulfide bonding by the removal of bound zinc that disrupts the folded structure, resulting in Hsp33 dimer formation (45). In tryparedoxin peroxidase in the thioredoxin superfamily, a difference in quaternary structure from dimer (oxidized form) to decamer (reduced form) has been observed, although with minor structural changes

[2] A. Vlamis-Gardikas and A. Holmgren, unpublished data.

Downloaded from www.jbc.org at Bibl Biologico-Medica, on April 2, 2012

within the thioredoxin domain (46). Oligomerization may well be part of the functionality of Grx4 even without inter-domain disulfides, considering the significant hydrophobic surfaces in the Grx4 structure, and the limited buffer conditions available for the current study. In monothiol glutaredoxins with only 1 cysteine in addition to that in the C*XFX* tetrad, a structural change on glutathionylation could induce mixed disulfide formation with specific targets or in oligomerization events. Indeed, such events could also be involved in folding/unfolding. Recently, *E. coli* thioredoxin and thioredoxin reductase were found to interact with unfolded and denatured proteins, in a manner similar to that of molecular chaperones that are involved in protein folding and protein renaturation after stress (47).

The present work describes the first solution structure of a natural monothiol glutaredoxin, Grx4, with high similarity to other members of this protein family, present in many living organisms and apparently essential. They have been shown to be involved in the formation of iron-sulfur clusters in proteins and to participate in antioxidant responses (6), and they may regulate signal transduction pathways by affecting the activity of protein kinases (20). The present study contributes to the molecular understanding of monothiol functionalities, in particular with regard to glutathionylation and disulfide formation. These molecular mechanisms form the basis for the role of monothiol glutaredoxins in the cellular defense against oxidative stress and relate monothiol glutaredoxins to atherosclerosis, aging, and Alzheimer's and Parkinson's diseases. Further studies of this protein family will be essential to fully understand their functionalities in the complete molecular environment of the cell.

Acknowledgment—Cecilia Andrésen (Linköping University) is gratefully acknowledged for expert advice concerning interpretation of the MALDI results. Professor Gottfried Otting and Dr. Edvards Liepinsh are acknowledged for generous advice regarding NMR experiments.

REFERENCES

1. Fernandes, A. P., and Holmgren, A. (2004) *Antioxid. Redox Signal.* **6,** 63–74
2. Vlamis-Gardikas, A., and Holmgren, A. (2002) *Methods Enzymol.* **347,** 286–296
3. Holmgren, A., Soderberg, B. O., Eklund, H., and Branden, C. I. (1975) *Proc. Natl. Acad. Sci. U. S. A.* **72,** 2305–2309
4. Jeng, M. F., Campbell, A. P., Begley, T., Holmgren, A., Case, D. A., Wright, P. E., and Dyson, H. J. (1994) *Structure* **2,** 853–868
5. Fernandes, A. P., Fladvad, M., Berndt, C., Andrésen, C., Lillig, C. H., Neubauer, P., Sunnerhagen, M., Holmgren, A., and Vlamis-Gardikas, A. (April 15, 2005) *J. Biol. Chem.* 10.1074/jbc.M500678200
6. Rodriguez-Manzaneque, M. T., Ros, J., Cabiscol, E., Sorribas, A., and Herrero, E. (1999) *Mol. Cell. Biol.* **19,** 8180–8190
7. Holmgren, A. (1976) *Proc. Natl. Acad. Sci. U. S. A.* **73,** 2275–2279
8. Tsang, M. L., and Schiff, J. A. (1978) *J. Bacteriol* **134,** 131–138
9. Shi, J., Vlamis-Gardikas, A., Åslund, F., Holmgren, A., and Rosen, B. P. (1999) *J. Biol. Chem.* **274,** 36039–36042
10. Sodano, P., Xia, T. H., Bushweller, J. H., Bjornberg, O., Holmgren, A., Billeter, M., and Wüthrich, K. (1991) *J. Mol. Biol.* **221,** 1311–1324
11. Lillig, C. H., Potamitou, A., Schwenn, J. D., Vlamis-Gardikas, A., and Holmgren, A. (2003) *J. Biol. Chem.* **278,** 22325–22330
12. Eklund, H., Ingelman, M., Soderberg, B. O., Uhlin, T., Nordlund, P., Nikkola, M., Sonnerstam, U., Joelson, T., and Petratos, K. (1992) *J. Mol. Biol.* **228,** 596–618
13. Åslund, F., Nordstrand, K., Berndt, K. D., Nikkola, M., Bergman, T., Ponstingl, H., Jörnvall, H., Otting, G., and Holmgren, A. (1996) *J. Biol. Chem.* **271,** 6736–6745
14. Sun, C., Berardi, M. J., and Bushweller, J. H. (1998) *J. Mol. Biol.* **280,** 687–701
15. Xia, B., Vlamis-Gardikas, A., Holmgren, A., Wright, P. E., and Dyson, H. J. (2001) *J. Mol. Biol.* **310,** 907–918
16. Yang, Y., Jao, S., Nanduri, S., Starke, D. W., Mieyal, J. J., and Qin, J. (1998) *Biochemistry* **37,** 17145–17156
17. Nordstrand, K., Åslund, F., Holmgren, A., Otting, G., and Berndt, K. D. (1999) *J. Mol. Biol.* **286,** 541–552
18. Bushweller, J. H., Åslund, F., Wüthrich, K., and Holmgren, A. (1992) *Biochemistry* **31,** 9288–9293
19. Belli, G., Polaina, J., Tamarit, J., De La Torre, M. A., Rodriguez-Manzaneque, M. T., Ros, J., and Herrero, E. (2002) *J. Biol. Chem.* **22,** 22
20. Witte, S., Villalba, M., Bi, K., Liu, Y., Isakov, N., and Altman, A. (2000) *J. Biol. Chem.* **275,** 1902–1909
21. Rodriguez-Manzaneque, M. T., Tamarit, J., Belli, G., Ros, J., and Herrero, E. (2002) *Mol. Biol. Cell* **13,** 1109–1121
22. Rahlfs, S., Fischer, M., and Becker, K. (2001) *J. Biol. Chem.* **276,** 37133–37140
23. Tamarit, J., Belli, G., Cabiscol, E., Herrero, E., and Ros, J. (2003) *J. Biol. Chem.* **278,** 25745–25751
24. Babichev, Y., and Isakov, N. (2001) *Adv. Exp. Med. Biol.* **495,** 41–45
25. Gerdes, S. Y., Scholle, M. D., Campbell, J. W., Balazsi, G., Ravasz, E., Daugherty, M. D., Somera, A. L., Kyrpides, N. C., Anderson, I., Gelfand, M. S., Bhattacharya, A., Kapatral, V., D'Souza, M., Baev, M. V., Grechkin, Y., Mseeh, F., Fonstein, M. Y., Overbeek, R., Barabasi, A. L., Oltvai, Z. N., and Osterman, A. L. (2003) *J. Bacteriol* **185,** 5673–5684
26. Szyperski, T., Guentert, P., Otting, G., and Wuethrich, K. (1992) *J. Magn. Reson.* **99,** 552–560
27. Ponstingl, H., and Otting, G. (1998) *J. Biomol. NMR* **12,** 319–324
28. Guntert, P., Dotsch, V., Wider, G., and Wüthrich, K. (1992) *J. Biomol. NMR* **2,** 619–629
29. Bartels, C., Xia, T., Billeter, M., Güntert, P., and Wüthrich, K. (1995) *J. Biomol. NMR* **5,** 1–10
30. Linge, J. P., O'Donoghue, S. I., and Nilges, M. (2001) *Methods Enzymol.* **339,** 71–90
31. Nilges, M., and O'Donoghue, S. I. (1998) *Progr. NMR Spectr.* **32,** 107–139
32. Cornilescu, G., Delaglio, F., and Bax, A. (1999) *J. Biomol. NMR* **13,** 289–302
33. Linge, J. P., Williams, M. A., Spronk, C., Bonvin, A., and Nilges, M. (2003) *Proteins Struct. Funct. Genet.* **50,** 496–506
34. Laskowski, R. A., Rullmannn, J. A., MacArthur, M. W., Kaptein, R., and Thornton, J. M. (1996) *J. Biomol. NMR* **8,** 477–486
35. Hooft, R. W., Vriend, G., Sander, C., and Abola, E. E. (1996) *Nature* **381,** 272
36. Koradi, R., Billeter, M., and Wüthrich, K. (1996) *J. Mol. Graph.* **14,** 51–55
37. Holm, L., and Sander, C. (1999) *Nucleic Acids Res.* **27,** 244–247
38. Gibrat, J. F., Madej, T., and Bryant, S. H. (1996) *Curr. Opin. Struct. Biol.* **6,** 377–385
39. Madej, T., Gibrat, J. F., and Bryant, S. H. (1995) *Proteins* **23,** 356–369
40. Sierk, M. L., and Pearson, W. R. (2004) *Protein Sci.* **13,** 773–785
41. Glaser, F., Pupko, T., Paz, I., Bell, R. E., Bechor-Shental, D., Martz, E., and Ben-Tal, N. (2003) *Bioinformatics* **19,** 163–164
42. Katti, S. K., Robbins, A. H., Yang, Y., and Wells, W. W. (1995) *Protein Sci.* **4,** 1998–2005
43. Holmgren, A. (1995) *Structure* **3,** 239–243
44. Burns, J. A., and Whitesides, M. (1990) *J. Am. Chem. Soc.* **112,** 6296–6303
45. Won, H. S., Low, L. Y., Guzman, R. D., Martines-Yamout, M., Jakob, U., and Dyson, H. J. (2004) *J. Mol. Biol.* **341,** 893–899
46. Alphey, M. S., Bond, C. S., Tetaud, E., Fairlamb, A. H., and Hunter, W. N. (2000) *J. Mol. Biol.* **300,** 903–916
47. Kern, R., Malki, A., Holmgren, A., and Richarme, G. (2003) *Biochem. J.* **371,** 965–972
48. Thompson, J. D., Higgins, D. G., and Gibson, T. J. (1994) *Nucleic Acids Res.* **22,** 4673–4680
49. Gouet, P., Courcelle, E., Stuart, D. I., and Metoz, F. (1999) *Bioinformatics* **15,** 305–308

Downloaded from www.jbc.org at Bibl Biologico-Medica, on April 2, 2012